ADS-B Signal Separation Via Complex Neural Network

Yue Yang[1], Haipeng Zhang[1], Haoran Zha[2(✉)], and Ruiliang Song[1]

[1] Beijing R&D Center, The 54th Research Institute of CETC, Beijing 100010, China
[2] Harbin Engineering University, Harbin 150001, China
zhahaoran@hrbeu.edu.cn

Abstract. In the sphere of air surveillance, the Automatic Dependent Surveillance-Broadcast is a valuable method. However, the ADS-B system suffers from a considerable overlap issue, and has a significant influence on signal decoding, resulting in incorrect decoding or even data loss. A complicated neural network-based separation approach for ADS-B overlap signals is presented in this paper. Taking the two-signal overlap as the research object, the simulation data set is generated. After the Hilbert transform of the overlap ADS-B signal, it is input into the complex neural network, and finally the predicted waveform of the source signal is output to realize ADS-B signal separation. Experiments have shown that the technique is more efficient and has a lower error rate than previously proposed algorithms.

Keywords: Blind source separation · ADS-B · Complex neural network · Hilbert transform

1 Introduction

As an important air surveillance technology, automatic dependent surveillance broadcast (ADS-B) has the capability of tracking aircrafts in civil aviation. When the aircraft initiates a transmission of relevant information such as altitude, speed, latitude, and others, the data link makes it available to others. Other aircrafts decode and obtain information when receiving these data, so as to realize global surveillance [1, 2]. For the time being, the majority of ADS-B systems are based on the ground-based ground station to monitor the airspace.

ADS-B on land faces the problem of signal overlap. When multiple signals collide and overlap at the receiver, the demodulation module will result in incorrect decoding or even loss of critical information, reducing the security and reliability of the surveillance system. To avoid this situation, the overlap signals must be separated and the separated signals must be decoded to obtain the correct information [3]. The methods provided by the ICAO document standard can only receive one correct signal, limiting surveillance capacity. Nicolas Petrohilos advocated the Projection Algorithm (PA) and Extended Projection Algorithm (EPA), which contributed significantly to the field of ADS-B signal separation [4–7]. Wang [8] used the Alternating Direction Method of Multipliers to the

J. Xiong et al. (Eds.): MobiMedia 2021, LNICST 394, pp. 679–688, 2021.
https://doi.org/10.1007/978-3-030-89814-4_49

nonconvex blind adaptive beamforming issue. FastICA can also separate overlap ADS-B signals under certain conditions [9].

Advances in deep learning have led to its widespread application in the analysis of anomalies, channel identification, and speech recognition [10–14]. More recently, deep learning-based modulation signal categorization algorithms have increased [15–17]. Zhang [18] applied the lightweight deep neural network to the modulation recognition of electromagnetic signals. Adversarial attack is also one of the most concerned research directions in the field of artificial intelligence security [19]. At present, the application of deep learning in the field of blind source separation is mostly limited in the separation of speech signals. Wang [20] applied deep learning to single channel speech signal separation, and achieved good results. The application of deep learning in ADS-B field is mainly used to classify ADS-B signals. Yang [21] used deep learning to classify ADS-B signals and ACARS signals. At present, the common deep learning is based on real value, and some recent studies show that complex numbers have more abundant feature representation ability than real numbers. Trabelsi established the deep complex convolution neural network (CV-CNN) for the first time in 2017. Tu [22] validates the superior performance in automatic modulation classification achieved by the complex-valued networks. Soorya [23] utilizes neural networks with complex weights to learn fingerprints. In this paper, the simulation ADS-B signal data set is generated, and the complex neural network is built. The signal after Hilbert transform is used as the input to get the estimated source signal.

2 Additional Background Knowledge

2.1 Signal Structure

This paper deals with the ADS-B signal in 1090 MHz format. The length of an ADS-B signal is typically 120 μs or 64 μs, This work focuses on the long signal, which has two different elements: an 8 μs preamble and a 112 μs data block. The preamble section contains four pulses of 0.5 μs length at 0 μs, 1 μs, 3.5 μs, and 4.5 μs, respectively. The data block of ADS-B signal is modulated by Pulse Position Modulation (PPM). Figure 1 depicts the structure of an ADS-B signal.

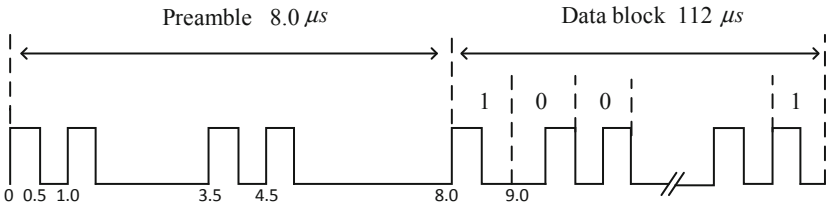

Fig. 1. ADS-B signal structure

2.2 Collision Pattern

Instead of requesting ahead of time, the ADS-B transmitter sends advisories and information depending on the pre-defined conditions and the state of the aircraft. Aircrafts spend the most of their time in the air in a constant condition. The aircraft is steady in the air, delivering 5.6 signals each second. The ADS-B signal is a bit sequence sent by each aircraft, and data from different planes will be delivered concurrently, resulting in signal overlap scenarios similar to the Aloha event. Because this collision mode accounts for the vast majority of occurrences, this study looks at what happens when two ADS-B signals collide.

3 Data Set Generation and Complex Neural Network

3.1 Data Set Generation

At present, it is hard to obtain effective measured data set of ADS-B overlap signal, so this paper has done a lot of related work on how to establish ADS-B signal data set. This study explores how to separate the overlap signals of two ADS-B signals, therefore generating all the overlap signals in the data set as a result of two ADS-B signals being seen to overlap in a given way under different situations.

Considering the difficulty and heavy workload of simulating the data sets in different signal time delay, different signal power difference and different SNR, the data set simulated in this paper is the overlap of two signals, and the time delay is 5 μs, 17 μs and 50 μs. The source signals' power differences are 2 dB, 3 dB, and 4 dB, respectively, the signal-to-noise ratio range is 5 dB–25 dB, and the interval step length is 5 dB. We first perform Hilbert transform on an ADS-B overlap signal, and then separate the real part from the imaginary part. The form of each signal stored in the data set can be regarded as the stitching of the real part and the imaginary part, in which the first half of each data is the real part, and the second half is the imaginary part. Among them, each data set is 90000 groups of signals, in which there are two source signals and one overlap signal. Figure 2 shows each signal in the dataset.

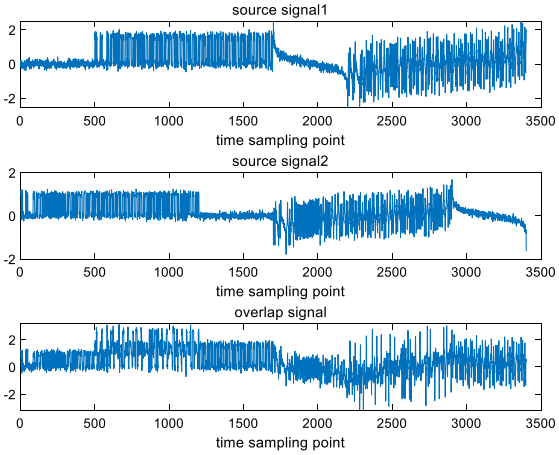

Fig. 2. Each group of signals in the dataset

3.2 Complex Neural Network

In order to realize the equivalent operation of 2D convolution in the complex domain, the complex filter matrix $\mathbf{h} = \mathbf{x} + i\mathbf{y}$ can be convoluted by the complex vector $\mathbf{W} = \mathbf{A} + i\mathbf{B}$.

$$\mathbf{W} * \mathbf{h} = (\mathbf{A} * \mathbf{x} - \mathbf{B} * \mathbf{y}) + i(\mathbf{B} * \mathbf{x} + \mathbf{A} * \mathbf{y}) \tag{1}$$

Figure 3 shows the schematic diagram of complex convolution operation, where M_I and M_R represent the imaginary part and real part characteristic graphs respectively, K_I and K_R represent the imaginary kernel and real kernel respectively.

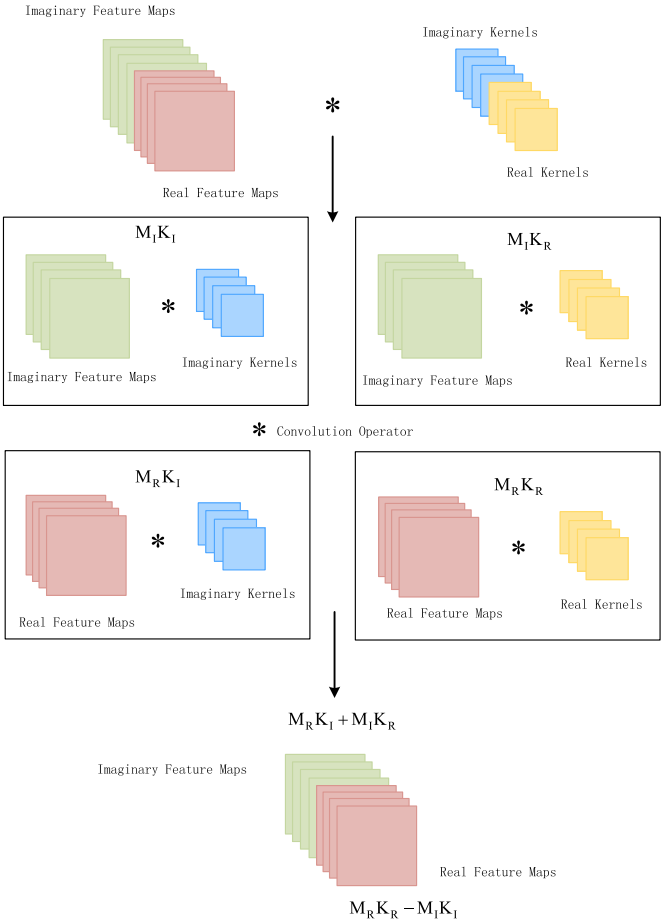

Fig. 3. Schematic diagram of complex convolution operation

In this paper, the real and imaginary parts of convolution operations are represented by matrix representation:

$$\begin{bmatrix} \Re(\mathbf{W} * \mathbf{h}) \\ \Im(\mathbf{W} * \mathbf{h}) \end{bmatrix} = \begin{bmatrix} \mathbf{A} & -\mathbf{B} \\ \mathbf{B} & \mathbf{A} \end{bmatrix} * \begin{bmatrix} \mathbf{x} \\ \mathbf{y} \end{bmatrix} \tag{2}$$

Batch normalization method can accelerate the learning speed of deep network, and batch normalization is very important for model optimization in some cases. However, because the standard formula of batch normalization is only applicable to real values, the batch normalization formula of complex values is adopted in this paper. Not only the input layer is normalized, but also the input of each middle layer is normalized.

In this paper, the problem is considered as a two-dimensional vector problem, which means that the data can be scaled according to the square root of the variance of the two principal components. This step can be completed by multiplying the 0-centered data $(\mathbf{x} - \mathbb{E}[\mathbf{x}])$ by the reciprocal of the square root of the 2×2 covariance matrix $\mathbf{V}$:

$$\widetilde{\mathbf{x}} = (\mathbf{V})^{-1/2}(\mathbf{x} - \mathbb{E}[\mathbf{x}]) \tag{3}$$

The normalization process can decorrelate the imaginary part and the real part of the element, which may avoid over fitting. This algorithm uses two parameters β and γ, in which the shift parameter β is a complex parameter and the scaling parameter γ is a 2×2 semi positive definite matrix.

Since the variance of real part and imaginary part of normalized input $\widetilde{\mathbf{x}}$ is 1, this chapter initializes γ_{rr} and γ_{ii} to $1/\sqrt{2}$, so that the variance modulus of normalized value is 1. Multiple batch normalization is defined as:

$$\mathrm{BN}(\widetilde{\mathbf{x}}) = \gamma\widetilde{\mathbf{x}} + \beta \tag{4}$$

In the training and testing process, the moving average with momentum is used to maintain the estimation of the normalized statistical data of the complex batch. The moving average values of V_{ri} and β are initialized to 0, the moving average values of V_{rr} and V_{ii} are initialized to $1/\sqrt{2}$, and the momentum of the moving average line is set to 0.9.

Proper weight initialization can avoid vanishing gradient. Therefore, the method of deriving complex weight parameters is as follows:

The complex weight has both polar and rectangular forms:

$$\mathbf{W} = |\mathbf{W}|e^{i\theta} = \Re\{\mathbf{W}\} + i\Im\{\mathbf{W}\} \tag{5}$$

where, θ and $|\mathbf{W}|$ is the phase and amplitude of $\mathbf{W}$.

4 Experiments

4.1 Experimental Setup

In the problem of data set selection, 5/6 of the data set is randomly selected as the training sample, 1/6 as the verification set and test sample for testing, and the data set is generated by random sampling.

In this experiment, the input of complex neural network is overlap signal waveform, and the output is two source signal waveforms predicted by complex neural network.

4.2 Evaluating Indicator

The evaluation indexes considered in this chapter are bit error rate and the similarity coefficient commonly used in traditional blind source separation. The definition of similarity coefficient is as follows:

$$\rho = \frac{\mathrm{cov}(x, y)}{\sqrt{\mathrm{cov}(x, x)\mathrm{cov}(y, y)}} \tag{6}$$

where, $\mathrm{cov}(x, y) = E\{[x - E(x)][y - E(y)]\}$ is the variance of x and y.

When the separated signal y approaches the source signal x, the similarity coefficient ρ approaches 1.

4.3 Experiment and Analysis

Experiment with the separation efficacy of overlap ADS-B signals by selecting two ADS-B signals at random, with a power difference of 3 dB between them, the time delay is 50 μs, and the SNR is 20 dB. Figure 4 shows the two original source signals as well as the overlap signals, and the input signal of neural network is shown in Fig. 5.

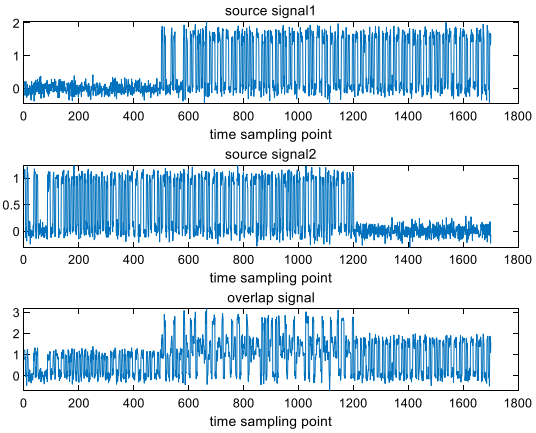

Fig. 4. Source signal and overlap signal

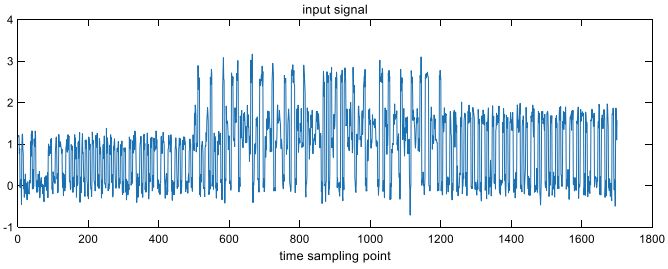

Fig. 5. Input signal of neural network

The output of the complex neural network is shown in Fig. 6. The real part of the intercepted output signal is shown in Fig. 7.

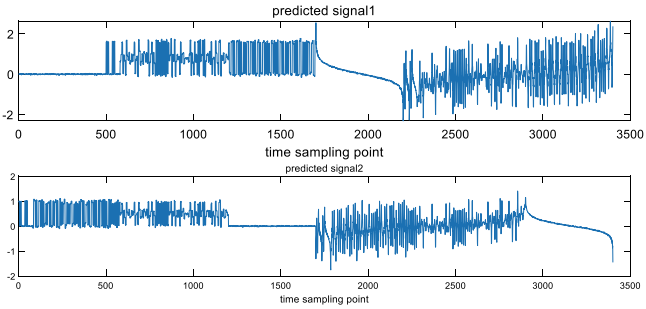

Fig. 6. Output signal of neural network

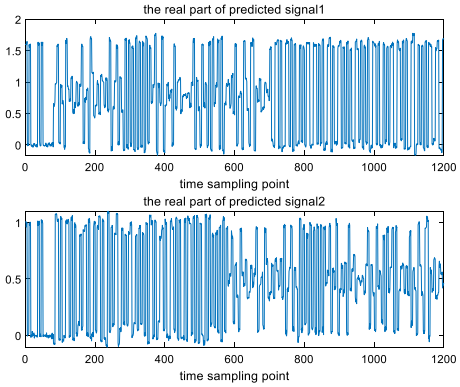

Fig. 7. Real part of output signal of neural network

As seen in Fig. 7, the actual sections of the two prediction signals generated by the complex neural network are comparable to the waveforms of the original signal in Fig. 6. It can be seen that complex neural network has the ability to separate ADS-B overlap signals.

The separation performance of the complex neural network is tested under the conditions that the two source signals have 2 dB, 3 dB, 4 dB power difference, the time latency between the two source signals is 5 μs, 17 μs and 50 μs, and the SNR is 5 dB, 10 dB, 15 dB, 20 dB and 25 dB.

When there is a 3 dB power differential between two signals and a 17 μs time delay, the curves of bit error rate of different algorithms vs SNR are presented in Fig. 8, and Table 1 shows the time consumption of different methods.

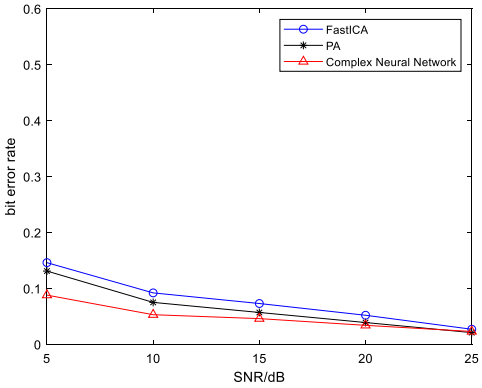

Fig. 8. Curve of bit error rate with SNR for different algorithms

Table 1. Separation time of different separation algorithms

Algorithm	Time (s)
FastICA	0.0419
PA	0.0828
Complex neural network	0.0014

As can be seen from Fig. 8, the complex neural network separation algorithm is better than traditional FastICA algorithm and PA algorithm. When the SNR is 5 dB and the power difference between the two ADS-B source signals is 3 dB, the BER is lower than 9%. It can be seen from Table 1 that the separation speed of the complex neural network reaches the millisecond level, which is significantly less than the other two algorithms.

When the two source ADS-B signals have different power differences, the curve of bit error rate changing with SNR is shown in Fig. 9, where the power differences are 2 dB, 3 dB and 4 dB; the SNR is 5 dB–25 dB. The similarity coefficient of separated waveform under different conditions is shown in Table 2.

This Fig. 9 shows that when the power difference between the source signals grows, the bit error rate drops. When the source signal has a power differential of 3 dB or 4 dB, the bit error rate is quite low. The greater the gap between the levels of the two sources, the less the influence on bit error rate is. Signal power difference sources increase in SNR, which causes the bit error rate of the same source signal power difference to drop simultaneously. When the power difference between the source signals is 4 dB and the SNR is 25 dB, the bit error rate is 1.8%. The similarity coefficient improves fast as the power difference between source signals and SNR grows. When the strength difference between source signals is 4dB, the similarity coefficient is 0.9314.

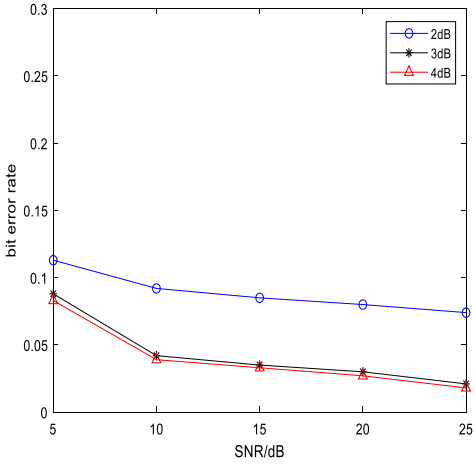

Fig. 9. Curve of bit error rate with SNR under different source signal power difference

Table 2. Similarity coefficient of separated waveform under different conditions

Power ratio	SNR				
	5 dB	10 dB	15 dB	20 dB	25 dB
2 dB	0.8053	0.8152	0.8474	0.8479	0.9203
3 dB	0.8782	0.9105	0.9127	0.9170	0.9230
4 dB	0.8860	0.9144	0.9181	0.9261	0.9314

5 Conclusion

This paper studies the application of deep learning in the separation of ADS-B overlap signals, and proposes a method of ADS-B signal separation based on complex neural network. The simulation data set is used in the experiment. The input of the complex neural network is the waveform of the overlap signal after Hilbert transform, and the output is the waveform of the two source signals predicted by the neural network after the Hilbert transform. The first half of each signal is the real part of the signal after Hilbert transform, and the second half is the imaginary part of the signal after Hilbert transform. Simulation results demonstrate that ADS-B signal separation algorithm based on complex neural network has better performance index, and bit error rate is lower than traditional algorithm. The time consumption reaches millisecond level, which can deal with large-scale signal overlap situation.

References

1. Strohmeier, M., Schafer, M., Lenders, V., Martinovic, I.: Realities and challenges of NexGen air traffic management: the case of ADSB. IEEE Commun. Mag. **52**(5), 111–118 (2014)

2. RTCA: Minimum operational performance standards for 1090 MHz extended squitter ADS-B, DO-260B, Washington, DC, pp. Appendix I (2009)
3. Werner, K., Bredemeyer, J., Delovski, T.: ADS-B over satellite: global air traffic surveillance from space. In: Tyrrhenian International Workshop on Digital Communications-Enhanced Surveillance of Aircraft and Vehicles, pp.47–52. IEEE (2014)
4. Petrochilos, N., van der Veen, A.-J.: Algorithms to separate overlapping secondary surveillance radar replies. In: 2004 IEEE International Conference on Acoustics, Speech, and Signal Processing, pp. 41–49. IEEE (2004)
5. Petrochilos, N., Piracci, E.G., Galati, G.N.: Separation of multiple secondary surveillance radar sources in a real environment for the near-far case. In: 2007 IEEE Antennas and Propagation Society International Symposium, pp. 3988–3991 (2007)
6. Petrochilos, N., Galati, G., Piracci, E.: Separation of SSR signals by array processing in multilateration systems. IEEE Tran. Aerosp. Eelctr. Syst. **45**(3), 965–982 (2009)
7. Petrochilos, N., van der Veen, A.-J.: Algebraic algorithms to separate overlapping secondary surveillance radar replies. IEEE Trans. Signal Process. **55**(7), 3746–3759 (2007)
8. Wang, W., Wu, R., Liang, J.: ADS-B signal separation based on blind adaptive beamforming. IEEE Trans. Veh. Technol. **68**(7), 6547–6556 (2019)
9. Zhang, Y., Li, W., Dou, Z.: Performance analysis of overlapping space-based ADS-B signal separation based on FastICA. In: 2019 IEEE Globecom Workshops (GC Wkshps), Waikoloa, HI, USA, pp. 1–6 (2019)
10. Zheng, D., You, F., Zhang, H., Gao, M., Jianzhi, Y.: Semantic segmentation method based on super-resolution. Int. J. Perform. Eng. **16**(5), 711–719 (2020)
11. Zhao, Y., et al.: Preserving minority structures in graph sampling. IEEE Trans. Vis. Comput. Graph. **27**(2), 1698–1708 (2021)
12. Lin, Y., Tu, Y., Dou, Z.: An improved neural network pruning technology for automatic modulation classification in edge devices. IEEE Trans. Veh. Technol. **69**(5), 5703–5706 (2020)
13. Gui, G., Liu, M., Tang, F., Kato, N., Adachi, F.: 6G: opening new horizons for integration of comfort, security, and intelligence. IEEE Wirel. Commun. **27**(5), 126–132 (2020)
14. Zhang, Z., Chang, J., Chai, M., Tang, N.: Specific emitter identification based on power amplifier. Int. J. Perform. Eng. **15**(3), 005–1013 (2019)
15. Lin, Y., Tu, Y., Dou, Z., Chen, L., Mao, S.: Contour Stella image and deep learning for signal recognition in the physical layer. IEEE Trans. Cogn. Commun. Netw. **7**(1), 34–46 (2021)
16. Jiabao, Y., Aiqun, H., Li, G., Peng, L.: A robust RF fingerprinting approach using multi-sampling convolutional neural network. IEEE Internet Things J. **6**(4), 6786–6799 (2019)
17. Lin, Y., Zhu, X., Zheng, Z., Dou, Z., Zhou, R.: The individual identification method of wireless device based on dimensionality reduction and machine learning. J. Supercomput. **75**(6), 3010–3027 (2017). https://doi.org/10.1007/s11227-017-2216-2
18. Zhang, S., Lin, Y., Tu, Y., et al.: Modulation recognition technology of electromagnetic signal based on lightweight deep neural network. J. Commun. **41**(11), 12–21 (2020)
19. Lin, Y., Zhao, H., Ma, X., Tu, Y., Wang, M.: Adversarial attacks in modulation recognition with convolutional neural networks. IEEE Trans. Reliab. **70**(1), 389–401 (2021)
20. Zhang, X.L., Wang, D.: A deep ensemble learning method for monaural speech separation. IEEE/ACM Trans. Audio Speech Lang. Process. **24**(5), 967–977 (2016)
21. Chen, S., Zheng, S., Yang, L., Yang, X.: Deep learning for large-scale real-world ACARS and ADS-B radio signal classification. IEEE Access **7**, 89256–89264 (2019)
22. Tu, Y., et al.: Complex-valued networks for automatic modulation classification. IEEE Trans. Veh. Technol. **69**(9), 10085–10089 (2020)
23. Gopalakrishnan, S., Cekic, M., Madhow, U.: Robust wireless fingerprinting via complex-valued neural networks. In: 2019 IEEE Global Communications Conference (GLOBECOM), Waikoloa, HI, USA, pp. 1–6 (2019)